

## DYNAMICS OF SINGULAR TRAVELING WAVE SOLUTIONS OF A SHORT CAPILLARY-GRAVITY WAVE EQUATION\*

Temesgen Desta Leta<sup>1,2,3</sup>, Wenjun Liu<sup>1,†</sup>  
and Abdelfattah El Achab<sup>4</sup>

**Abstract** In this paper, dynamical behaviour of traveling wave solutions to a short capillary-gravity equation is analyzed by using the method of bifurcation. When the phase orbits intersects the singular parabola  $y^2 = 2\phi/\lambda$  on the phase plane, then the trajectories create a weaker wave fronts than the regular traveling wave solutions. By using proper Euler transformations, we reformulate the model as a singular chaotic problem, which can then be analyzed using the singularity study. We prove existence of three types of physically realistic traveling wave solutions to the case of small diffusion for the first time, two-peaked solitary waves, three-peaked and multi-peaked periodic wave solutions.

**Keywords** Singular parabola, singular periodic wave solutions, multi-peaked periodic wave solutions, two-peaked solitary wave solutions.

**MSC(2010)** 24C23, 24K18, 37C27, 37C29.

### 1. Introduction

Recently, studies on time dependent nonlinear wave equations of dynamical systems which describe many important phenomena in computational sciences, biology, astrophysics, etc., have become a central theme of researchers. A shallow water wave for small amplitude on a long-surface wave and an intermediate wave has produced a lot of interesting and remarkable nonlinear wave equations [8, 9]. For example, the Green Naddhi system, Benjamin-Bona-Mahony-Peregrine equation and Boussinesq or modified Boussinesq equations exhibits a smooth traveling

---

<sup>†</sup>The corresponding author. Email: [wjliu@nuist.edu.cn](mailto:wjliu@nuist.edu.cn) (W. Liu)

<sup>1</sup>School of Mathematics & Statistics, Nanjing University of Information Science and Technology, Nanjing 210044, China

<sup>2</sup>Reading Academy, Nanjing University of Information Science and Technology, Nanjing 210044, China

<sup>3</sup>Department of Mathematics, Dilla University, 419, Dilla, Ethiopia

<sup>4</sup>Department of Mathematics, Faculty of Sciences, University Cadi Ayyad Bd. du Prince Moulay Abdellah, B.P. 2390 Marrakech, Morocco

\*The first author is supported by the Talented Young Scientist Program of Ministry of Science and Technology of China (Ethiopia -18-010) and the National Natural Science Foundation of China (No. 11950410502). The second author is supported by the National Natural Science Foundation of China (No. 11771216) and the Six Talent Peaks Project in Jiangsu Province (No. 2015-XCL-020).

wave solution on intermediate waves arising from a purely nonlinear diffusive flux term [1, 11, 12, 20]. Another class of models are the Korteweg and de Vries (KdV) and the Camassa and Holm (CH) equations with nonlinear dispersion which address traveling waves in long-wave dynamics resulting from a combined diffusive and advective flux term [4, 14]. If the effect of dispersion on the motion of the wave is reduced, the wave fronts become peak-like traveling wave solutions and for the detailed basic theory on singular solutions for a class of traveling wave equations, we would like to recommend the reader to refer [6, 7, 10, 13, 18, 21].

Manna and Neveu in [19] studied the following integrable model from a (2+1)-dimensional asymptotic dynamics of a short capillary-gravity wave

$$u_{xt} = \frac{3g(1-3\theta)}{2vh}u - \frac{1}{2}uu_{xx} - \frac{1}{4}u_x^2 + \frac{3h^2}{4v}u_{xx}u_x^2, \quad (1.1)$$

where  $u(x, t)$  is the fluid velocity on the surface,  $x$  and  $t$  are space and time variables. They concluded that, true peaks of traveling wave solutions arising from the interaction of nonlinear dispersion terms of the model are results of these singularity behaviours or discontinuities. After appropriately rescaling the variables of Eq. (1.1) Borzi & *et al* in [2] studied and modified Eq. (1.1) to the form of

$$u_{xt} = u - uu_{xx} - \frac{1}{2}u_x^2 + \frac{\lambda}{2}u_{xx}u_x^2, \quad (1.2)$$

which was used to describe short capillary-gravity waves. A Lax pair and finite time singularity for Eq (1.2) was provided by Manna and Neveu in [19] and multivalued solutions in finite time were argued based on a map to the Sine-Gordon equation.

More recently, Chen & *et al* in [5] studied the effect of singular quadratic curves on the singularity of traveling wave solutions and showed that Eq. (1.1) has a new kind of singular periodic wave solution if the corresponding periodic orbits are tangent to the parabola in the phase plane. However, the authors only obtained an implicit expression of singular periodic wave solutions for a spacial case, that is  $\lambda = 1$  in Eq. (1.2). Besides, the phase portraits of bifurcations of the corresponding traveling wave system were incomplete. The purpose of this paper is to study the dynamical behaviour of a short capillary-gravity wave with surface tension using bifurcation method and to find the exact traveling wave solutions of a second-order singular traveling wave solution with singular parabolic curve.

This paper is organized as follows. In Sec. 2, the generation of dynamical systems and bifurcations of the phase portraits of Eq. (1.2) depending on the changes of parameter  $(\rho, \lambda, h)$  are discussed. In Sec. 3, main results on classification of the traveling wave solutions with all possible exact parametric representations of solutions is studied. The last section is devoted to some final remarks.

## 2. Dynamical systems and phase portrait analysis

To study the traveling wave solution of Eq. (1.2), we let  $u(x, t) = \phi(\xi) + \rho$ ,  $\xi = x - \rho t$  where  $\rho$  is the wave speed, then Eq. (1.2) can be transformed to the following traveling wave equation

$$-\rho\phi_{\xi\xi} - (\phi + \rho) + (\phi + \rho)\phi_{\xi\xi} + \frac{1}{2}\phi_{\xi}^2 - \frac{\lambda}{2}\phi_{\xi\xi}\phi_{\xi}^2 = 0, \quad (2.1)$$

that can be written in Hamiltonian system as

$$\frac{d\phi}{d\xi} = y, \quad \frac{dy}{d\xi} = \frac{\phi + \rho - \frac{1}{2}y^2}{\phi - \frac{\lambda}{2}y^2}. \quad (2.2)$$

Since for  $\phi = \frac{\lambda}{2}y^2$ , the right hand-side of the second equation of system (2.2) is discontinuous and it accounts for the nonuniqueness of some traveling wave solutions, which we call *singular traveling wave system of the second class* (see [15–17]). Eq. (2.2) admits weak traveling wave solutions with peaks, cusps and solitary solutions with compact support. The system (2.2) has a parabola singular curves  $\phi = \frac{\lambda}{2}y^2$ . Once integrating system (2.2) we have

$$H(\phi, y) = -4(\phi + 2\rho)\phi + 4\phi y^2 - \lambda y^4 = h. \quad (2.3)$$

System (2.3) is a planer dynamical system defined in two parameter space  $(\rho, \lambda)$ . Imposing the transformation  $d\xi = (\phi - \frac{\lambda}{2}y^2) d\zeta$ , for  $\phi \neq \frac{\lambda}{2}y^2$  on system (2.2) leads to the following associated regular system

$$\frac{d\phi}{d\zeta} = \left(\phi - \frac{\lambda}{2}y^2\right) y = \frac{\partial H}{\partial y}, \quad \frac{dy}{d\zeta} = \phi + \rho - \frac{1}{2}y^2 = -\frac{\partial H}{\partial \phi}. \quad (2.4)$$

Because the phase orbits defined by the vector fields of system (2.4) determine all traveling wave solutions, we will investigate the bifurcations of phase portraits of this system in phase plane  $(\phi, y)$  as the parameters are changed.

Obviously, if  $\rho(1 - \lambda) \leq 0$ , system (2.4) has only one equilibrium point  $E(\phi_\rho, 0)$  where  $\phi_\rho = -\rho$ . If  $\rho(1 - \lambda) > 0$ , system (2.4) has three equilibrium points  $E_\rho(\phi_\rho, 0)$ ,  $S_\pm(\phi_s, \pm y_s)$  where,  $\phi_s = \frac{\rho\lambda}{1-\lambda}$  and  $y_s = \sqrt{\frac{2\rho}{1-\lambda}}$ . Let  $M(\phi, y)$  be the coefficient matrix of the linearized system of (2.4) at an equilibrium point  $(\phi, y)$ . We have  $J(\phi_\rho, 0) = \det M(\phi_\rho, 0) = -\phi_\rho = \rho$  and  $J(\phi_s, \pm y_s) = \det M(\phi_s, \pm y_s) = -2\rho$ . Based on the theory of planar dynamical system, for an equilibrium point of a planar integrable system, the equilibrium point is a saddle point if  $J < 0$ ; the equilibrium point is a center point (a node point) if  $J > 0$  and  $(trM)^2 - 4J < (>)0$ ; the equilibrium point is a cusp, if  $J = 0$  and the Poincaré index of the equilibrium point is 0. We write for  $H(\phi, y)$  given by (2.3),  $h_1 = H(\phi_\rho, 0) = 4\rho^2$ ;  $h_2 = H(\phi_s, \pm y_s) = -\frac{4\lambda\rho}{1-\lambda}$ .

To do a qualitative analysis from the above information, we have the following five different cases of system (2.2) depending on the parameter group  $(\rho, \lambda)$ .

**Case 1. Assume that**  $\rho > 0, \lambda < 0$ . In this case, for  $0 < h_1 < h_2$ , the equilibrium point  $E(\phi_\rho, 0)$  is a center. System (2.2) has a two real zeros  $\phi_{A_1} = \rho - \frac{1}{2}\sqrt{4\rho^2 - h}$  and  $\phi_{B_1} = \rho + \frac{1}{2}\sqrt{4\rho^2 - h}$  and also intersects longitudinally (see Fig 1 (b)) with the parabola  $y^2 = \frac{2}{\lambda}\phi$  at two points,  $K_\pm(\phi_k, \pm y_k)$ , where  $\phi_k = \frac{\rho(\lambda - \sqrt{-\lambda})}{1-\lambda}$  and  $y_k = \sqrt{2\phi_k}$ . We have the phase orbits shown in Fig. 1.

**Case 2. Assume that**  $\rho < 0, 0 < \lambda < 1$ . Corresponding to the level curve defined by  $H(\phi, y) = h$ ,  $h \in (h_2, h_0)$ , has a global periodic orbit enclosing the equilibrium point  $C_3(\phi_\rho, 0)$  intersecting the singular parabola  $y^2 = \frac{2}{\lambda}\phi$  at  $A_\pm(\phi_1, \pm y_1)$ , where  $\phi_1 = 2\rho/(1 + \lambda)$  (see Fig. 2(a)). The level curve defined by  $H(\phi, y) = 0$ , there exists two symmetric homoclinic orbit, connecting the saddle point  $E(\phi_\rho, 0)$ , intersect with the singular parabola at four points  $A_\pm(\phi_1^*, \pm y_1^*)$  and  $C_{2,4}(\phi_2^*, \pm y_2^*)$ , where  $\phi_1^* = -\rho\sqrt{\lambda}/(1 - \sqrt{\lambda})$  and  $\phi_2^* = \rho\sqrt{\lambda}/(1 - \sqrt{\lambda})$  (see Fig. 2(b)). We have the phase portrait shown in Fig. 2(a)–(c).

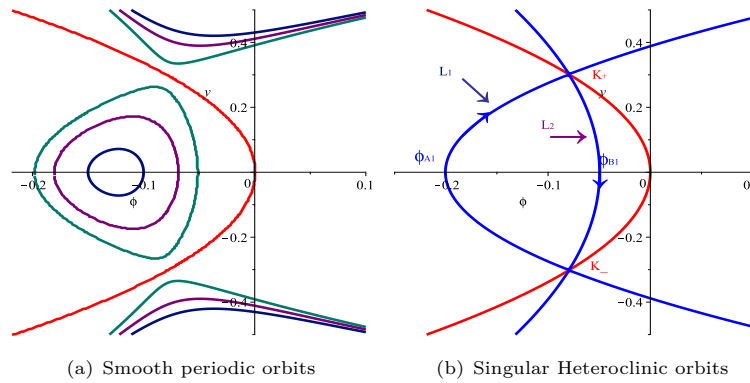


Figure 1. Bifurcations of phase portraits of system (2.2) when  $\rho > 0$  and  $\lambda < 0$ .

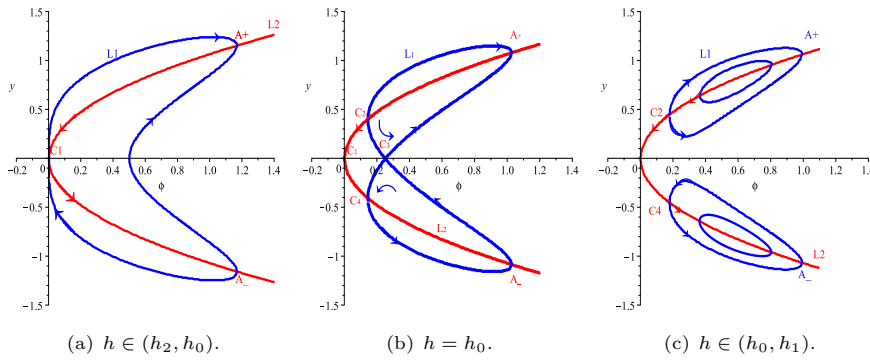


Figure 2. Bifurcations of phase portraits of system (2.2) when  $\rho < 0$  and  $\lambda > 0$ .

**Case 3. Assume that  $\rho < 0, \lambda = 0$ .** In this case,  $h_2 = 0$ , the level curve defined by  $H(\phi, y) = h$ , has a pair of open orbits intersecting with the parabola  $y^2 = \frac{2}{\lambda}\phi$  at exactly two points  $S_{\pm}(\phi_s, \pm y_s)$ . The equilibrium point  $E(\phi_{\rho}, 0)$  is a saddle point and Eq (2.3) we obtained a kink and anti-kink wave solution at  $E(\phi_{\rho}, 0)$ . We have the phase portrait shown in Fig 3.

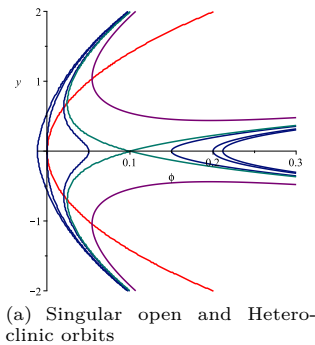


Figure 3. Bifurcations of phase portraits of system (2.2) when  $\rho < 0$  and  $\lambda \geq 0$ .

**Case 4. Assume that  $\rho > 0, \lambda = 0$ .** In this case system (2.2) can be rewritten as

$$\frac{d\phi}{d\xi} = y; \quad \frac{dy}{d\xi} = \frac{\phi + \rho - 1/2y^2}{\phi}, \tag{2.5}$$

with the first integral

$$H^*(\phi, y) = \phi(\phi + 2\rho) + \phi y^2 = h^*. \tag{2.6}$$

Here for  $\phi = 0$ , the right hand-side of equation of (2.5) is discontinuous and its some traveling wave solutions are perturbed. Consider the subcases (a)  $\rho < 0$ , Fig 4(a), (b)  $\rho = 0$ , Fig 4(b), (c)  $\rho > 0$ , Fig 4(c) given below.

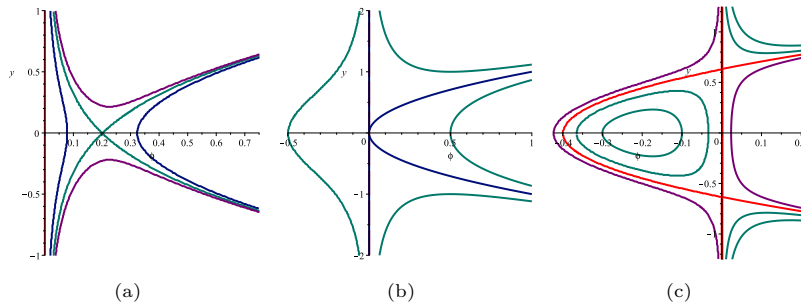


**Figure 4.** Bifurcations of phase portraits of system (2.2) when  $\rho \rightarrow 0$  and  $\lambda = 0$ .

**Case 5. Assume that  $\rho > 0, \lambda > 0$ .** In this case we have  $h_2 < 0 < h_1 < \infty$ . Consider four different phase portraits given under here. The level curve defined by  $H(\phi, y) = h_s = \frac{\lambda\rho}{1-\lambda}$ , has two heteroclinic orbits intersecting with the parabola  $y^2 = \frac{2}{\lambda}\phi$  at the points  $S_+$  and  $S_-$ , (see Fig 5 (a)), we call singular heteroclinic orbit. The two orbits intersect with the  $\phi$ - axis at the points  $A_1(\phi_{A_1}, 0)$  and  $A_2(\phi_{A_2}, 0)$  respectively, where  $\phi_{A_1} = -\rho + \frac{\rho}{\sqrt{2(1-\lambda)}}$  and  $\phi_{A_2} = -\rho - \frac{\rho}{\sqrt{2(1-\lambda)}}$ .

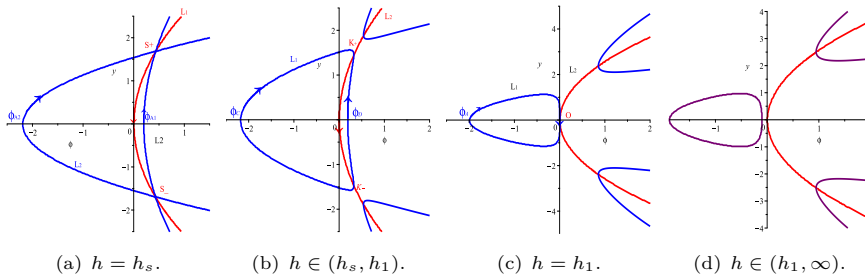


**Figure 5.** Bifurcations of phase portraits of system (8) when  $\rho > 0$  and  $\lambda > 0$ .

Corresponding to the level curves defined by  $H(\phi, y) = h, h \in (h_s, h_1)$ , there exists a singular periodic orbit connecting the parabola at  $(\phi_{B_2}, \pm\sqrt{2\phi_{B_2}})$  where  $\phi_{B_2} = \sqrt{\frac{-h}{8\rho}}$ , see Fig. 5(b). For  $h = h_1$ , there is a singular periodic orbit intersecting with the  $y^2 = 2/\lambda\phi$  at the origin  $O(0, 0)$ . For Fig. 5(d), we have a family of periodic orbits that has no intersection with our parabola. This family of periodic orbits

gives rise a family of smooth periodic wave solutions of Eq. (1.2). In the next section we shall give exact singular traveling wave solutions of system (2.2) based on bifurcation theory.

### 3. Main Results

It is noted for the aforementioned five cases there exist intersection points between the phase orbits and the singular curve. At these intersection points two possible contrary directions can be found for the trajectory of system (2.2). When a trajectory along a homoclinic orbit moves at a intersection point on the singular curve, it forms a peak type soliton. Next, we will describe the evolution of traveling wave solutions for these cases basing on the phase orbits.

#### 3.1. Existence of smooth and singular periodic wave solutions

i) For  $\rho > 0, \lambda < (> 0)$ , the level curve defined by the Hamiltonian  $H(\phi, y) = h, h \in (0, h_1)$ , there exist a periodic orbit that has no intersection point with the parabola  $y^2 = \frac{2}{\lambda}\phi$  (see Fig 1(a) and Fig. 5(d)). Thus, (2.2) has family of smooth periodic wave solutions. The algebraic equation of periodic orbit is given by

$$\left(\frac{d\phi}{d\xi}\right)^2 = \frac{1}{\lambda} \left(2\phi \pm \sqrt{4(1-\lambda)\phi^2 - (8\rho\phi + h)\lambda}\right), \quad (3.1)$$

where the sign  $\pm$  before the term  $\sqrt{4(1-\lambda)\phi^2 - (8\rho\phi + h)\lambda}$  is independent on the interval of  $\phi$  and intersects with the  $\phi$ - axis at two points  $\phi_{A_1}$  and  $\phi_{B_1}$ . Thus, from Eq. (3.1) and the first equation of system (2.2), we have the following parametric representation for the periodic orbit:

$$\Gamma_1 = \int_{\phi}^{\phi^-} \frac{\sqrt{\lambda}d\phi}{\sqrt{2\phi - \sqrt{4(1-\lambda)\phi^2 - (8\rho\phi + h)\lambda}}} \quad (3.2)$$

and

$$|\xi - 2n\Gamma_1| = \int_{\phi}^{\phi^-} \frac{\sqrt{\lambda}d\phi}{\sqrt{2\phi - \sqrt{4(1-\lambda)\phi^2 - (8\rho\phi + h)\lambda}}}, \quad (3.3)$$

where  $|\xi - 2n\Gamma_1| \leq \Gamma_1$ . Consequently, along this orbit when  $\phi \rightarrow 0$ , one may have  $\frac{d\phi}{d\xi} \rightarrow 0, \frac{d^2\phi}{d\xi^2} \rightarrow \pm\infty$ . When,  $h \rightarrow 0$ , the smooth periodic wave advances into a singular periodic wave. We simulated the singular traveling wave solution by Maple and shown in Fig. 6(a)–(c).

For  $h = 0$ , the periodic orbit is tangent to the parabola  $y^2 = \frac{2}{\lambda}\phi$ , at the origin  $O(0,0)$  (see Fig. 5(c)). The corresponding periodic wave solution satisfies

$$\left(\frac{d\phi}{d\xi}\right)^2 = \frac{1}{\lambda} \left(2\phi \pm \sqrt{4(1-\lambda)\phi^2 - 8\rho\phi\lambda}\right), \quad (3.4)$$

and

$$\left(\frac{d^2\phi}{d\xi^2}\right)^2 = \frac{\left(4\rho\lambda + 4(1-\lambda)\phi + \sqrt{-4\phi(\lambda-1)\phi + 2\rho\lambda}\right)^2}{\phi\lambda(2\rho\lambda + (1-\lambda)\phi)}. \quad (3.5)$$

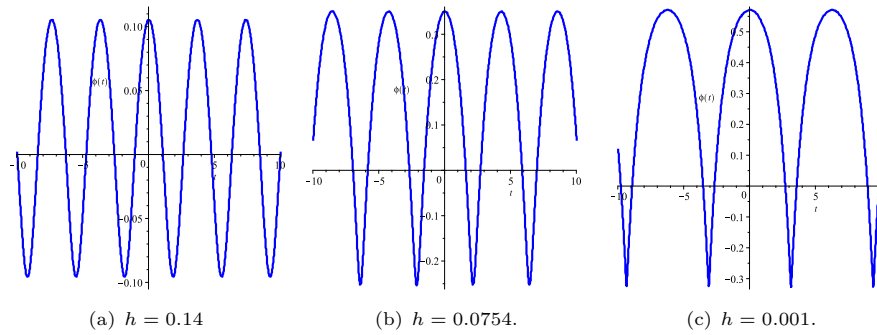


**Figure 6.** As  $h \rightarrow 0$ , a smooth periodic wave evolved into singular periodic wave.

Now, by applying a substitution  $(\psi\phi)^2 = 4(1-\lambda)\left(\phi^2 + \frac{8\rho\lambda\phi}{1-\lambda}\right)$  into Eq. (3.1) gives rise  $\tilde{y}^2 = \frac{(2-\psi)(\psi^2-4(1-\lambda))^3}{32\rho\lambda^2\psi^2}$ . Then by the first equation of system (2.2), we have

$$\int_{\psi}^{\psi^*} \frac{\psi d\psi}{(\psi^2-4(1-\lambda))\sqrt{(2-\psi)(\psi^2-4(1-\lambda))}} = \int_{\psi}^{\psi^*} \frac{R(\psi)d\psi}{\sqrt{(2-\psi)(\psi^2-4(1-\lambda))}}$$

$$= -\frac{|\xi|}{4\lambda\sqrt{2\rho}} \tag{3.6}$$

where,  $R(\psi) = \frac{\psi}{\psi^2-4(1-\lambda)}$ . Therefore, we obtain the following parametric representation of singular periodic wave solutions of Eq. (2.2) ( see Fig 6(c)):

$$\phi(\chi) = \frac{32\rho\lambda}{\psi^2(\chi)-4(1-\lambda)}, \quad \psi(\chi) = \frac{(2-A)+(A+2)\text{cn}(\chi,k)}{1+\text{cn}(\chi,k)},$$

$$\xi(\chi) = \sqrt[4]{\frac{A(1-\lambda)}{\rho^2}} \left\{ \chi - \sqrt{1-\lambda}\Pi(\arccos(\text{cn}(\chi,k)), \alpha^2, k) \right. \tag{3.7}$$

$$\left. - \sqrt{1-\lambda}\Pi\left(\arccos\left(\frac{2-A}{2+A}\right), \alpha^2, k\right) \right\},$$

where,  $A = 2\sqrt{4(1-\lambda)^2-1}$ ,  $k^2 = \frac{A-2}{A} < \alpha^2 < 1$  where  $\text{cn}(\chi, k)$  is Jacobean elliptic function described in (see [3]).

### 3.2. Weak kink-peakon and weak antikink-peakon interacted singular traveling wave solutions associated with heteroclinic orbit

It is well known that a heteroclinic orbit on the phase plane corresponds to a kink and anti-kink traveling wave solution, for the orbit not intersecting with the singular curve as  $\xi$  increases. For  $h_1 = 4\rho^2$ ,  $\lambda = 1$  we have two paths passing through the intersection points or saddle points  $K_-$  and  $K_+$ , we call them  $L_1$  and  $L_2$  (see Fig. 1(b)). For the vector field moving from  $K_- \rightarrow \phi_{A_1} \rightarrow K_+ \rightarrow \phi_{B_1} \rightarrow K_-$ , we have a heteroclinic orbit with the type of kink and anti-kink singular wave solutions are obtained.

Now, from Eq. (3.1) we have a heteroclinic orbit which can be expressed in the following form:

$$\frac{1}{\sqrt{\lambda}}\xi = \int_{\phi}^{\phi^*} \frac{d\phi}{\sqrt{2\phi \pm \sqrt{4(1-\lambda)\phi^2 - (8\rho\phi + h)\lambda}}}. \tag{3.8}$$

By using a long calculation with scale transformation and substituting  $\phi = -(4\rho^2 - \psi^2)/8\rho$  into Eq. (3.6) and by the first equation of system (2.2) we get an improper integral of the form

$$\xi = \int_{\psi}^{\psi^*} \frac{\psi d\psi}{4\rho\sqrt{\psi + \frac{4\rho^2 - \psi^2}{4\rho}}}, \quad \psi^* \in (\phi_{A_1}, \phi_{B_1}). \tag{3.9}$$

Hence, we have obtain the following parametric representation of weak kink-peakon interacted and weak antikink-peakon singular traveling wave solution of Eq. (1.2) (see Fig. 7(a) and (b)):

$$\phi(\xi) = \pm \left( \frac{4\rho^2 + \psi^2(\xi)}{8\rho} \right), \tag{3.10}$$

and

$$\frac{\sqrt{-\psi(\xi)^2 + 4\psi(\xi)\rho + 4\rho^2}}{2\sqrt{\rho}} \pm \sqrt{\rho} \arctan \left( \frac{\psi(\xi) - 2\rho}{\sqrt{-\psi(\xi)^2 + 4\psi(\xi)\rho + 4\rho^2}} \right) = 4\rho\xi + \sqrt{\rho} + \rho\pi. \tag{3.11}$$

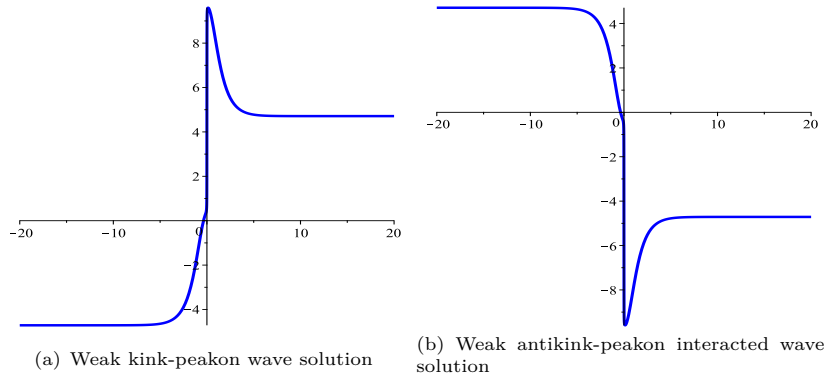


Figure 7. Wave profile corresponding to exact wave solution of Eq. (3.10).

### 3.3. Existence of singular periodic and two-peaked solitary wave solutions

i) Consider Fig. 2(a). When  $\rho < 0, \lambda > 0$ , for each  $H(\phi, y) = h, h \in (-\infty, h_1)$  there exists a global singular periodic orbit intersects the  $\phi$ -axis at  $(\phi_p, 0)$  and also intersects the parabola  $y^2 = \frac{2}{\lambda}\phi$ , at  $E_{1,2}(\pm\phi_1, \pm y_1)$ , where  $\phi_1 = \frac{2\rho}{2+\lambda}$  and  $y_1 = \sqrt{\frac{2}{\lambda}\phi_1}$ . Thus, for  $\lambda = 1$ , the parabola intersecting the periodic orbit divides

the path into three segments, different combinations of which forms the following three types of waves.

a) For the trajectory moves as  $\Gamma_1 : C_1 \rightarrow A_+ \xrightarrow{Jump} C_1$ , then from Eq. (3.1) we have

$$y^2 = 2\phi + \sqrt{-8\phi\rho - h}. \tag{3.12}$$

b) For trajectory moving through the points  $\Gamma_2 : A_+ \xrightarrow{Jump} C_1 \xrightarrow{Jump} A_- \rightarrow A_+$ , then from Eq. (3.1) we have

$$y^2 = 2\phi - \sqrt{-8\phi\rho - h}. \tag{3.13}$$

c) For trajectory moving through  $\Gamma_3 : C_1 \xrightarrow{Jump} A_- \rightarrow C_1$ , then from Eq. (3.1) we have

$$y^2 = -2\phi - \sqrt{-8\phi\rho - h}. \tag{3.14}$$

From the above three subcases, we concluded that the parabola  $y^2 = 2\phi$ , has an effect on the existence of singular periodic wave solutions. Now, from Eq. (3.1) we have  $\psi^2 = -8\phi\rho - h$ , then  $\phi = -\frac{h+\psi^2}{8\rho}$ ,  $\psi_A = (2\rho\sqrt{-h} - 8\rho^2 - h)^{\frac{1}{2}}$  as  $\phi_A = \frac{4\rho - \sqrt{-h}}{4}$ ,  $\psi_B = \sqrt{-h}$ , as  $\phi = -\rho$ . Thus from Eq. (3.12)-(3.14) we have

$$\tilde{y}^2 = \left(\frac{d\psi}{d\xi}\right)^2 = \frac{4\rho(\psi - \psi_A)(\psi_B - \psi)}{\psi^2}. \tag{3.15}$$

Now, by using Eq. (3.12) and the first equation of system (2.2), we have the following first integral

$$2\sqrt{\rho}\xi = \int_{\psi_{A-}}^{\psi} \frac{\psi d\psi}{\sqrt{(\psi - \psi_A)(\psi_B - \psi)}}. \tag{3.16}$$

Hence, corresponding to the level curve  $\widehat{A_+C_1A_-}$ , Eq. (1.2) have a parametric representation of a multi-peaked singular periodic wave solution (see Fig. 9(a)):

$$\phi(\xi) = -\frac{h + \psi^2(\xi)}{8\rho} \tag{3.17}$$

and

$$\psi(\xi) = \left(\frac{\psi_A - \psi_B}{2}\right) + \left(\frac{\psi_A + \psi_B}{2}\right) \sinh(2\sqrt{\rho}\xi), \quad \xi \in \left[\operatorname{arcsinh}\left(\frac{2\phi_1(\psi_B - \psi_A)}{\psi_A + \psi_B}\right), \frac{\pi}{2}\right]. \tag{3.18}$$

Corresponding to the level curves defined by  $H(\phi, y) = h$ ,  $h \in (-\infty, h_1)$ , of the trajectories  $\widehat{C_1A_+C_1}$  and  $\widehat{C_1A_-C_1}$  from Eq. (3.13) and (3.14) respectively, we have the following first integrals:

$$\int_{\psi_0}^{\psi} \frac{\psi d\psi}{\sqrt{(\psi - \psi_A)(\psi_B - \psi)}} = 2\sqrt{\rho}\xi \tag{3.19}$$

and

$$-\int_{\psi_0}^{\psi} \frac{\psi d\psi}{\sqrt{(\psi - \psi_A)(\psi_B - \psi)}} = 2\sqrt{\rho}\xi. \tag{3.20}$$

Therefore, corresponding to (3.19) and (3.20), we have a parametric representation of singular periodic wave solution for Eq. (1.2) given by:

$$\phi(\xi) = \frac{h + \psi^2}{8\rho}; \tag{3.21}$$

$$\psi(\xi) = \left(\frac{\psi_A - \psi_B}{2}\right) + \left(\frac{\psi_A + \psi_B}{2}\right) \sinh(2\sqrt{\rho}\xi), \quad \xi \in \left[-\frac{\pi}{2}, \operatorname{arcsinh}\left(\frac{2\phi_1(\psi_B - \psi_A)}{\psi_A + \psi_B}\right)\right];$$

and

$$\psi(\xi) = \left(\frac{\psi_B - \psi_A}{2}\right) - \left(\frac{\psi_A + \psi_B}{2}\right) \sinh(2\sqrt{\rho}\xi), \quad \xi \in \left[-\frac{\pi}{2}, -\operatorname{arcsinh}\left(\frac{2\phi_1(\psi_A - \psi_B)}{\psi_A + \psi_B}\right)\right]. \tag{3.22}$$

**Theorem 3.1** (The Rapid Jump Property of  $y = d\phi/d\xi$  when the singular parabola intersecting a periodic orbit). *If the singular parabolic curve intersects with a family of periodic orbit at the singularity points  $A_+$  and  $A_-$ , the periodic waves have pairs of opposite vector fields. Let  $(\phi, y = d\phi/d\xi)$  be a point on the periodic orbit  $\Gamma_1$  of (2.2). Then, along  $\Gamma_1$  to the singular parabolic curve  $y^2 = (2/\lambda)\phi$ ,  $y = d\phi/d\xi$  jumps down rapidly to  $A_-$  in a very short time interval of  $\xi$ . The periodic wave solution (3.7) is different from the well-known smooth periodic wave solution, i.e., as  $h \rightarrow h_s$ , the first derivative  $d\phi/d\xi$  exists while the second derivative  $d^2\phi/d\xi^2$  doesn't exist at the equilibrium point. We call this periodic wave solution singular periodic wave solution.*

ii) Consider Fig. 2(b). Corresponding to the level curve defined by  $H(\phi, y) = h_1 = 4\rho^2$ , there exists a two symmetric homoclinic orbits, connecting the saddle point  $E(\phi_\rho, 0)$ , and intersects with the parabola  $y^2 = \frac{2}{\lambda}\phi$ , at four points  $A_\pm(\phi_{1^*}, \pm y_{1^*})$  and  $C_{2,4}(\phi_{2^*}, \pm y_{2^*})$ . As the trajectories on the phase plane intersects with the singular curve, different moves can be explored with the increasing of the parameter  $\xi$ , i.e.,  $A_+ \xrightarrow{Jump} C_2 \rightarrow C_3 \rightarrow A_+$ ,  $A_+ \xrightarrow{Jump} C_2 \rightarrow C_3 \rightarrow C_4 \xrightarrow{Jump} A_- \rightarrow C_3 \rightarrow A_+$ ,  $A_+ \xrightarrow{Jump} C_2 \rightarrow C_3 \rightarrow C_4 \xrightarrow{Jump} C_2 \rightarrow A_+$ ,  $C_3 \rightarrow C_4 \xrightarrow{Jump} C_2 \rightarrow C_3$ , and etc. In the following part we shall discuss the dynamical behaviour of the waves associated with the phase portrait and the parabola intersecting at  $C_4$  and/or  $C_2$ , which forms a peak on the waves and jumps between those points. In the following parts we shall discuss the different peaked solitary wave solutions determined from these moves.

a) Consider the trajectory defined by the wave  $A_+ \xrightarrow{Jump} C_2 \rightarrow C_3 \rightarrow A_+$ , which forms two peak forms of periodic wave solutions. In this case we can consider three different motions of the wave forms  $\widehat{A_+C_2}$ ,  $\widehat{C_2C_3}$  and  $\widehat{C_3A_+}$ . From Eq. (3.1) we have

$$\Gamma_1 = \widehat{A_+C_2} : y^2 = \frac{1}{\lambda} \left(2\phi + \sqrt{4(1-\lambda)\phi^2 - (8\rho\phi + h_1)\lambda}\right), \quad \phi \in (\phi_{1^*}, \phi_{2^*}], \tag{3.23}$$

$$\Gamma_2 = \widehat{C_2C_3} : y^2 = \frac{1}{\lambda} \left(2\phi - \sqrt{4(1-\lambda)\phi^2 - (8\rho\phi + h_1)\lambda}\right), \quad \phi \in [\phi_{2^*}, \phi_\rho], \tag{3.24}$$

$$\Gamma_3 = \widehat{C_3A_+} : y^2 = \frac{1}{\lambda} \left(2\phi - \sqrt{4(1-\lambda)\phi^2 - (8\rho\phi + h_1)\lambda}\right), \quad \phi \in (\phi_\rho, \phi_{1^*}]. \tag{3.25}$$

Using the transformation  $\phi \rightarrow \phi_{1^*} - \phi_{2^*}$ , when  $\psi(\xi_0) = \phi_\rho \rightarrow 0$ ,  $\psi_{1^*} \rightarrow \frac{4\rho^2(\lambda-1)+\rho\lambda}{\lambda-1}$ , when  $\phi \rightarrow \phi_{1^*}$ ,  $\psi_{2^*} \rightarrow -\frac{4\rho^2(\lambda-1)+\rho\lambda}{\lambda-1}$ , when  $\phi \rightarrow \phi_{2^*}$ . From system

(3.25) letting

$$(\psi(\phi - \phi_\rho))^2 = 4(1 - \lambda)\phi^2 - (8\rho\phi + h_1)\lambda,$$

we have two sets of solutions of  $\phi(\xi)$  and its first derivatives with respect to the curve  $\Gamma_1$  and  $\Gamma_2$  respectively:

$$\phi(\xi) = \frac{\phi_s\psi(\xi)^2 + 4(\lambda - 1)\phi_s - 4\rho\lambda}{\psi(\xi)^2 + 4\lambda - 4}, \quad \frac{d\phi}{d\xi} = \frac{8\rho\lambda\psi(\xi)}{(\psi(\xi)^2 + 4\lambda - 4)^2} \frac{d\psi}{d\xi}, \quad (3.26)$$

and

$$\phi(\xi) = -\frac{\phi_s\psi(\xi)^2 + 4(\lambda - 1)\phi_s - 4\rho\lambda}{\psi(\xi)^2 + 4\lambda - 4}, \quad \frac{d\phi}{d\xi} = -\frac{8\rho\lambda\psi(\xi)}{(\psi(\xi)^2 + 4\lambda - 4)^2} \frac{d\psi}{d\xi}. \quad (3.27)$$

From Eq. (3.26), Eq. (3.27) and the first equation of system (2.2) we have respectively

$$\begin{aligned} \Gamma_1 &= \int_{\psi}^{\psi_{2^*}} \frac{\psi d\psi}{\sqrt{(\psi_\rho + \psi)^2 (\psi^2 + 4\lambda - 4)^3}} = \int_{\psi}^{\psi_{2^*}} \frac{\psi d\psi}{(\psi_\rho + \psi)(\psi^2 + 4\lambda - 4)\sqrt{\psi^2 + 4\lambda - 4}} \\ &= \frac{1}{2\lambda} \sqrt{\frac{1}{\rho\lambda(\lambda - 1)}} \int_0^\xi d\xi, \end{aligned} \quad (3.28)$$

$$\begin{aligned} \Gamma_2 &= \int_{\psi_{2^*}}^{\psi} \frac{\psi d\psi}{\sqrt{(\psi_\rho - \psi)^2 (\psi^2 + 4\lambda - 4)^3}} = \int_{\psi_{2^*}}^{\psi} \frac{\psi d\psi}{(\psi_\rho - \psi)(\psi^2 + 4\lambda - 4)\sqrt{\psi^2 + 4\lambda - 4}} \\ &= \frac{1}{2\lambda} \sqrt{\frac{1}{\rho\lambda(\lambda - 1)}} \int_{\xi^*}^\xi d\xi = -\Gamma_3, \end{aligned} \quad (3.29)$$

where  $\xi^* = 2\lambda\sqrt{\rho\lambda(\lambda - 1)} \int_{\psi_{2^*}}^{\psi} \frac{\psi d\psi}{(\psi_\rho - \psi)(\psi^2 + 4\lambda - 4)\sqrt{\psi^2 + 4\lambda - 4}}$ .

Thus, by using a long mathematical computation on Eqs. (3.28) and (3.29), we have a parametric representation of multi-peaked periodic wave solution for  $\Gamma_1$  given as follows (see Fig 8(a)):

$$\phi(\xi) = \frac{\phi_s\psi(\xi)^2 + 4(\lambda - 1)\phi_s - 4\rho\lambda}{\psi(\xi)^2 + 4\lambda - 4}; \quad (3.30)$$

and

$$\frac{2(1 - \lambda) + \psi}{2\lambda\sqrt{\rho\lambda(\lambda - 1)}\sqrt{\psi^2 + 4\lambda - 4}} + \frac{1}{2\sqrt{\rho\lambda}} \ln\left(\frac{4(1 - \lambda)\psi - 8(\lambda - 1)}{2(1 + \lambda)\psi}\right) = 0, \quad (3.31)$$

and corresponding to  $\Gamma_2$  and  $\Gamma_3$  we have a parametric representation of given:

$$\phi(\xi) = -\frac{\phi_s\psi(\xi)^2 + 4(\lambda - 1)\phi_s - 4\rho\lambda}{\psi(\xi)^2 + 4\lambda - 4}; \quad (3.32)$$

and

$$\frac{2(1 - \lambda) - \psi}{2\lambda\sqrt{\rho\lambda(\lambda - 1)}\sqrt{\psi^2 + 4\lambda - 4}} + \frac{1}{2\sqrt{\rho\lambda}} \ln\left(\frac{-4(1 - \lambda)\psi - 8(\lambda - 1)}{2(1 + \lambda)\psi}\right) = 0. \quad (3.33)$$

b) For the phase orbit moving through  $A_+ \xrightarrow{Jump} C_2 \rightarrow C_3 \rightarrow C_4 \xrightarrow{Jump} A_- \rightarrow C_3 \rightarrow A_+$ , we have a solitary wave with two peaks can be obtained. From Eq. (3.1) and the first equation of system (2.2) we have

$$\Gamma_s = \int_{\phi_{1^*}}^{\phi_{2^*}} \frac{d\phi}{\sqrt{2\phi - \sqrt{4(1-\lambda)\phi^2 - (8\rho\phi + h)\lambda}}}, \quad (3.34)$$

$$\xi - \xi_0 = \int_{\phi_{1^*}}^{\phi} \frac{d\phi}{\sqrt{2\phi - \sqrt{4(1-\lambda)\phi^2 - (8\rho\phi + h)\lambda}}}, \quad \xi \in (\xi_0, \Gamma_s + \xi_0); \quad (3.35)$$

$$\xi - \xi_0 = \Gamma_s + \int_{\phi_{2^*}}^{\phi} \frac{d\phi}{\sqrt{2\phi + \sqrt{4(1-\lambda)\phi^2 - (8\rho\phi + h)\lambda}}}, \quad \xi \in (\Gamma_s + \xi_0, +\infty). \quad (3.36)$$

In this case the peak exists at  $\xi = \xi_0$  and at  $\xi = \xi_0 + \Gamma_s$  respectively (see Fig. 8(b)).

c) For the phase orbit moving through  $A_+ \xrightarrow{Jump} C_2 \rightarrow C_3 \rightarrow C_4 \xrightarrow{Jump} C_2 \rightarrow A_+$ , we have a solitary wave with three peaks can be found. From Eq. (3.1) and the first equation of system (2.2) we have

$$\Gamma_s = \int_{\phi_{1^*}}^{\phi_{2^*}} \frac{d\phi}{\sqrt{2\phi + \sqrt{4(1-\lambda)\phi^2 - (8\rho\phi + h)\lambda}}}, \quad (3.37)$$

$$\xi - \xi_0 = \int_{-\phi_{1^*}}^{\phi} \frac{d\phi}{\sqrt{2\phi + \sqrt{4(1-\lambda)\phi^2 - (8\rho\phi + h)\lambda}}}, \quad \xi \in (\xi_0, \Gamma_s + \xi_0), \quad (3.38)$$

$$\xi - \xi_0 = \Gamma_s + \int_{\phi_{1^*}}^{\phi} \frac{d\phi}{\sqrt{2\phi + \sqrt{4(1-\lambda)\phi^2 - (8\rho\phi + h)\lambda}}}, \quad \xi \in (\Gamma_s + \xi_0, 2\Gamma_s + \xi_0), \quad (3.39)$$

$$\xi - \xi_0 = 2\Gamma_s + \int_{\phi_{2^*}}^{\phi} \frac{d\phi}{\sqrt{2\phi - \sqrt{4(1-\lambda)\phi^2 - (8\rho\phi + h)\lambda}}}, \quad \xi \in (2\Gamma_s + \xi_0, +\infty). \quad (3.40)$$

In this case three peaks exists at  $\xi = \xi_0$ ,  $\xi = \Gamma_s + \xi_0$  and at  $\xi = \xi_0 + 2\Gamma_s$  respectively (see Fig. 8(c)).

d) For the phase orbit moving through  $C_3 \rightarrow C_4 \xrightarrow{Jump} C_2 \rightarrow C_3$ , we have a peakon wave solution can be found. From Eq. (3.1) and the first equation of system (2.2) we have

$$\Gamma_s = \int_{-\phi_{2^*}}^{\phi} \frac{d\phi}{\sqrt{2\phi - \sqrt{4(1-\lambda)\phi^2 - (8\rho\phi + h)\lambda}}},$$

$$\xi - \xi_0 = \int_{-\phi_{2^*}}^{\phi} \frac{d\phi}{\sqrt{2\phi - \sqrt{4(1-\lambda)\phi^2 - (8\rho\phi + h)\lambda}}}, \quad \xi \in (-\infty, +\infty). \quad (3.41)$$

In this case the peak exists at  $\xi = \xi_0$ , (see Fig. 8(d)).

iii) Consider Fig. 2(c). In this case the level curve defined by  $H(\phi, y) = h$ ,  $h \in (h_1, \infty)$ , there exists a two families of periodic orbits intersecting the parabola  $y^2 = \frac{2}{\lambda}\phi$  at four points  $A_+$ ,  $C_2$ ,  $C_4$  and  $A_-$ , and divide each family of periodic orbits in two pairs of segments. We observe that, as  $\xi$  varies along the periodic orbits

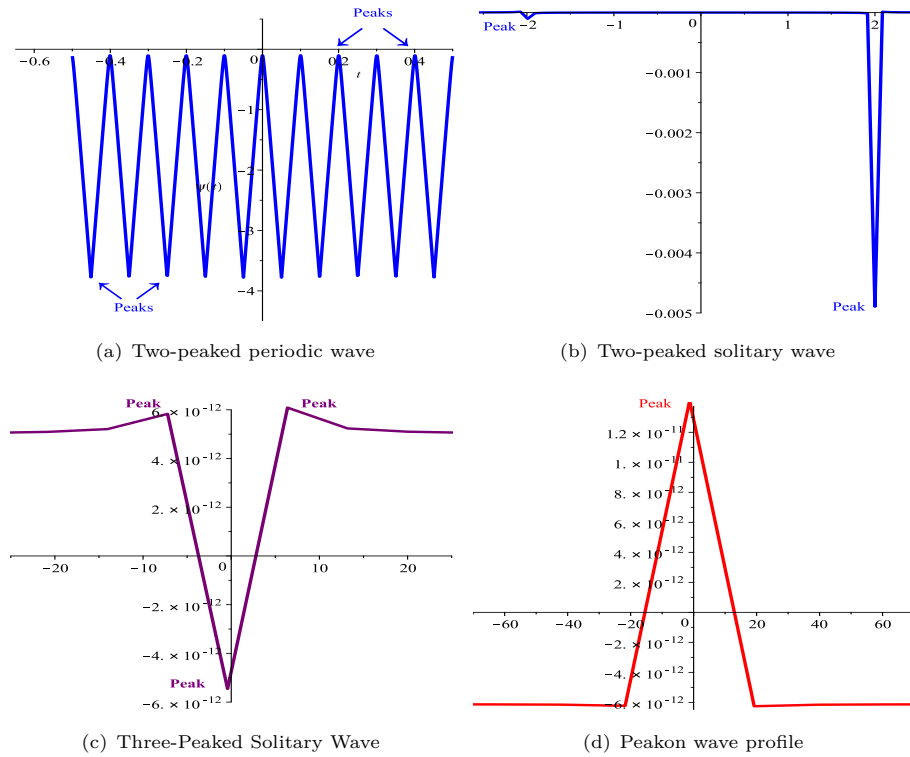


Figure 8. Wave profiles of system (2.2)

of system (4), there exists two opposite directions of vector field at each point of intersection and the phase portraits creates a singular periodic orbits which are different from the well known smooth periodic wave solutions. In this case, the singular periodic wave solution is a weak solution of system (2.2) which has a continuous first derivative, while the second derivative at the equilibrium point vanish.

### 3.4. Existence of breaking, peakon and anti-peakon wave solutions

In this case we consider Fig 4(a)–(c) for any  $\rho$  and  $\lambda \rightarrow 0$ .

(i) Corresponding to  $\rho < 0$ , in Fig. 4(a), we have a family of open orbits defined by  $H^*(\phi, y) = h^*$ ,  $h^* \in (h_2, 0)$ , intersecting at  $E(\phi_\rho, 0)$ . From system (2.5), we have

$$\xi = \int_{\phi_\rho}^{\phi} \frac{\sqrt{\phi} d\phi}{\sqrt{h^* \phi - \phi(\phi + 2\rho)}} = \int_{\phi_\rho}^{\phi} \frac{\sqrt{\phi} d\phi}{\sqrt{G(\phi)}}. \tag{3.42}$$

Thus, we have a parametric representation of a breaking wave solution for system (2.5) (see Fig. 9 (a)):

$$\begin{aligned} \phi(\chi) &= \phi_L + \frac{\phi_\rho - \phi_L}{1 + \left(\frac{\phi_\rho - \phi_L}{\phi_L}\right) \text{sn}^2(\omega\chi, k)}; \\ \xi(\chi) &= \phi_\rho \sqrt{\phi_L} \left[ \sqrt{\frac{\phi_L}{\phi_\rho}} (E(\text{am}(\omega\chi, k), k) - k^2 \text{sn}(\omega\chi, k) \text{cd}(\omega\chi, k)) \right], \end{aligned} \tag{3.43}$$

where  $\chi \in \left[ \sin^{-1} \sqrt{\frac{\phi_\rho \phi_L}{\phi_L - \phi_\rho} - \frac{1}{2}} \right)$ ,  $k = \sqrt{1 - \frac{\phi_\rho}{\phi_L}}$ ,  $\omega = \frac{1}{\sqrt{\phi_L}}$ .

(ii) For  $\rho = 0$ , in Fig. 4(b), the level curve defined by  $H^*(\phi, y) = 0$ , we have an open curve intersecting the singular straight line  $\phi = 0$ , forming a pair of stable and unstable manifolds at  $A_\pm(0, \pm\sqrt{2\rho})$ , we call a singular Heteroclinic orbit, which gives the known kink and anti-kink wave solution as  $\xi \rightarrow \pm\infty$ .

(iii) Corresponding to the third subcase  $\rho > 0$ , Fig 4(c), has an energy level defined by  $H(\phi, y) = h$ ,  $h \in (h_0, h_1)$ , we have a family of periodic orbits enclosing the equilibrium point  $E(-\phi_\rho, 0)$ . For  $h = h_1 = h_s$ , system (2.5) have a two families of heteroclinic orbits connecting the equilibrium points  $(0, \pm y_s)$ . In this case we have  $G(\phi) = \phi(\phi - \phi_m)$ . Hence we have a peakon and anti-peakon wave solution (see Fig 9 (b) and (c)):

$$\phi = \phi_m + \exp(\pm 2\xi). \tag{3.44}$$

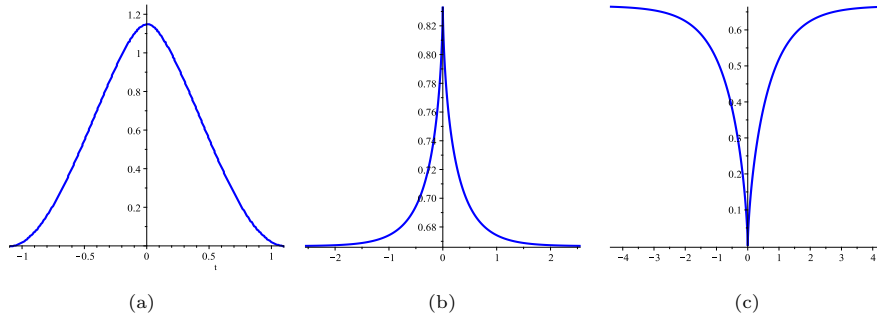


**Figure 9.** Traveling wave solution of system (2.5). 9(a) A breaking wave of Eq. (3.43); 9(b) A peakon wave solution and 9(c) An anti-peakon wave solution of Eq. (3.44)

### 3.5. Existence of solitary and multi-peak periodic wave solution

The level curve defined by  $H(\phi, y) = h_s = \frac{4\rho^2}{1-\lambda}$ , has two heteroclinic orbits intersecting with the parabola  $y^2 = \frac{2}{\lambda}\phi$  at the saddle points  $S_+$  and  $S_-$ , we call singular heteroclinic orbit. As show in Fig. 5(a), the two orbits intersect with the  $\phi$ - axis at the points  $A_1(\phi_{A_1}, 0)$  and  $A_2(\phi_{A_2}, 0)$  respectively, where  $\phi_{A_1} = -\rho + \frac{\rho\sqrt{\lambda}}{\sqrt{1-\lambda}}$  and  $\phi_{A_2} = -\rho - \frac{\rho\sqrt{\lambda}}{\sqrt{1-\lambda}}$ . Corresponding to the associated regular system (2.4) have two solitary wave solutions for slow time motion  $\zeta$  (see Fig 10(a)) while for system (2.2), it is noted that the two saddle points gives rise to singular periodic wave solution with multi-peak (see Fig 10 (b)). From Eq. (3.1) and for  $\phi \in [\phi_A, \phi_S]$  and  $\phi \in [\phi_B, \phi_S]$ , respectively we have

$$\widehat{S_-AS_+} : y^2 = \frac{1}{\lambda} \left( 2\phi + \sqrt{4(1-\lambda)\phi^2 - (8\rho\phi + h)\lambda} \right) = \frac{2(1-\sqrt{1-\lambda}) \left( \phi - \sqrt{\lambda}\phi_{A_1} \right)}{\lambda}, \tag{3.45}$$

and

$$\widehat{S_-BS_+} : y^2 = \frac{1}{\lambda} \left( 2\phi - \sqrt{4(1-\lambda)\phi^2 - (8\rho\phi + h)\lambda} \right) = \frac{2(1 + \sqrt{1-\lambda})(\phi - \sqrt{\lambda}\phi_{A_2})}{\lambda}. \tag{3.46}$$

From Eq. (3.45), (3.46) and the first equation of system (2.2) we have

$$\int_{\phi_{S_-}}^{\phi} \frac{d\phi}{\sqrt{\phi - \sqrt{\lambda}\phi_{A_1}}} = \sqrt{\frac{\lambda}{2(1 - \sqrt{1-\lambda})}} |\xi - 2nT|, \quad n \in \mathbb{Z}, \tag{3.47}$$

where  $|\xi - 2nT| \leq T$  and

$$T = \sqrt{\frac{2(1 - \sqrt{1-\lambda})}{\lambda}} \int_{\phi_{S_-}}^{\phi_{S_+}} \frac{d\phi}{\sqrt{\phi - \sqrt{\lambda}\phi_{A_2}}}. \tag{3.48}$$

Therefore, we obtain the following exact parametric representations of singular periodic wave solutions of Eq. (1.2)

$$\phi_a(\xi) = \phi_{A_1} + \frac{1 - \sqrt{1-\lambda}}{2\lambda} (\xi - 2nT)^2, \quad |\xi - 2nT| \leq T, \tag{3.49}$$

$$\phi_b(\xi) = \phi_{A_2} + \frac{1 + \sqrt{1-\lambda}}{2\lambda} (\xi - (2n+1)(T+T_1))^2, \quad |\xi - (2n+1)(T+T_1)| \leq T_1. \tag{3.50}$$

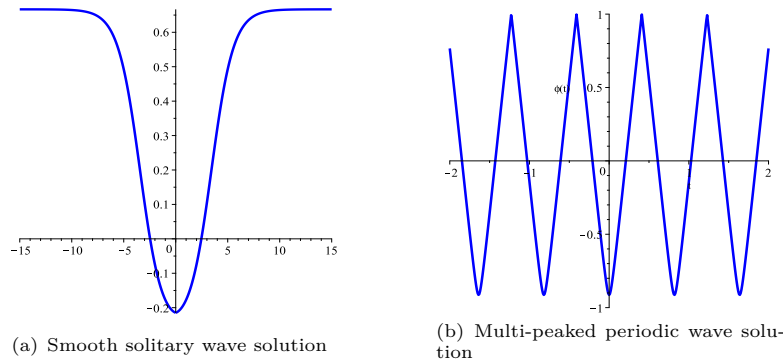


**Figure 10.** As  $h$  goes from  $h_0 \rightarrow h_s$ , the smooth solitary wave evolves into a singular periodic wave.

### 4. Conclusion

It is well-known that a homoclinic orbit corresponds a smooth solitary wave solution, a heteroclinic orbit corresponds to a kink wave solution. Similarly, a periodic orbit corresponds to a smooth periodic wave solutions. However, when the homoclinic orbit, heteroclinic orbit, or periodic orbit intersects with the singular parabola in the phase plane, things will get complicated. In fact, the existence of two opposite directions of vector field at each intersection points leads to the jump between the intersection points, and thus the occurrence of new types of singular waves

containing peaks (i.e., two-peaked and three-peaked solitary wave solutions and multi-peaked periodic wave solutions (see Eq. (3.17), Eq. (3.30), Eq. (3.31), Eq. (3.44), Eq. (3.49), Eq. (3.50)) and the two singular periodic wave solutions are obtained (see Eq. (3.9) and Eq. (3.21)), in which both of which are not found in [5]. To sum up, we have proved the following Theorems.

**Theorem 4.1.** *When the homoclinic orbit intersects with the singular parabola, with the increase  $\xi$ , the trajectory no longer passing across the intersection points along the orbit, may jump between the intersection points  $A_+$ , and  $A_-$  or  $C_2$  and  $C_4$ , and gives rise a different types of peaked solitary wave solution. It is shown that the second derivatives of the new singular solitary wave solutions does not exists.*

**Theorem 4.2.** *When the a heteroclinic orbits intersect with the singular curve, it gives rise a weak kink and anti-kink wave solution (3.10) which is different from the well known smooth kink and anti-kink wave solution.*

## References

- [1] T. B. Benjamin, J. L. Bona and J. J. Mahony, *Model equations for long waves in nonlinear dispersive systems*, Philos. Trans. R. Soc. London, Ser. A, 1972, 272, 47–78.
- [2] C. H. Borzi, R. A. Kraenkel, M. A. Manna and A. Pereira, *Nonlinear dynamics of short traveling capillary-gravity waves*, Phys. Rev. E, 2005, 71, 0263071–9.
- [3] P. F. Byrd and M. D. Fridman, *Handbook of Elliptic Integrals for Engineers and Scientists*, Springer, Berlin, 1971.
- [4] R. Camassa and D. D. Holm, *An integrable shallow water equation with peaked solitons*, Phys. Rev. Lett., 1993, 71, 1661–1664.
- [5] A. Chen and et al. *Effects of quadratic singular curves in integrable equations*, Stud.Appl. Math., 2015, 134, 24–61.
- [6] A. Das and A. Ganguly, *Existence and stability of dispersive solutions to the Kadomtsev-Petviashvili equation in the presence of dispersion effect*, Commun. Nonlin. Sci. Numer. Simulat, 2017, 48, 326–339.
- [7] A. Das, N. Ghosh and K. Ansari, *Bifurcation and exact traveling wave solutions for dual power Zakharov-Kuznetsov-Burgers equation with fractional temporal evolution*, Comp. & Math. with Appl., 2018, 75(1), 59–69.
- [8] H. R. Dullin, G. Gottwald and D. D. Holm, *An integrable shallow water equation with linear and non-linear dispersion*, Phys. Rev. Lett., 2001, 87, 4501–4504.
- [9] A. S. Fokas and Q. Liu, *Asymptotic integrability of water waves*, Phys. Rev. Lett., 1996, 77, 2347–2351.
- [10] A. Geyer and M. Víctor, *Singular solutions for a class of traveling wave equations arising in hydrodynamics*, NonlinearAnal. RWA, 2016, 31, 57–76.
- [11] A. E. Green, N. Laws and P. M. Naghdi, *On the theory of water waves*, Proc. R. Soc. London, Ser. A, 1974, 338, 43–55.
- [12] A. E. Green and P. M. Naghdi, *A derivation of equations for wave propagation in water of variable depth*, J. Fluid Mech., 1976, 78, 237–246.

- 
- [13] R. Hakl and M. Zamora, *Periodic solutions to second-order indefinite singular equations*, J. Differential Equations, 2017, 263(1), 451–469.
- [14] D. Korteweg and G. de Vries, *On the change of form of long waves advancing in a rectangular channel and a new type of long stationary waves*, Philos. Mag., 1895, 39, 422–443.
- [15] T. D. Leta and J. Li, *Dynamical behavior of traveling wave solutions of a long waves-short waves resonance model*, Qual. Theory Dyn. Syst., 2018, 27, 1750129.
- [16] J. Li, *Singular Nonlinear Traveling Wave Equations: Bifurcations and Exact Solutions*, Science, Beijing, 2013.
- [17] J. Li and G. Chen, *On a class of singular nonlinear traveling wave equations*, Int. J. Bifurcation and Chaos, 2007, 17, 4049–4065.
- [18] M. A. Manna and V. Merle, *Modified Korteweg-De Vries hierarchies in multiple-time variables and the solutions of modified Boussinesq equations*, Proc Math. Phys. Engin. Sci., 1998, 454, 1445–1456.
- [19] M. A. Manna and A. Neveu, *A singular integrable equation from short capillary-gravity waves*, preprint arXiv: physics/0303085(2003) 1-4.
- [20] O. Nwogu, *Alternative form of Boussinesq equations for near shore wave propagation*, J. Waterway, Port, Coastal, Ocean Engng, ASCE, 1993, 119, 618–638.
- [21] R. A. Seadawy, D. Lu and M. A. Khater, *Bifurcations of solitary wave solutions for the three dimensional Zakharov-Kuznetsov-Burgers equation and Boussinesq equation with dual dispersion*, Optik, 2017, 143, 104–114.